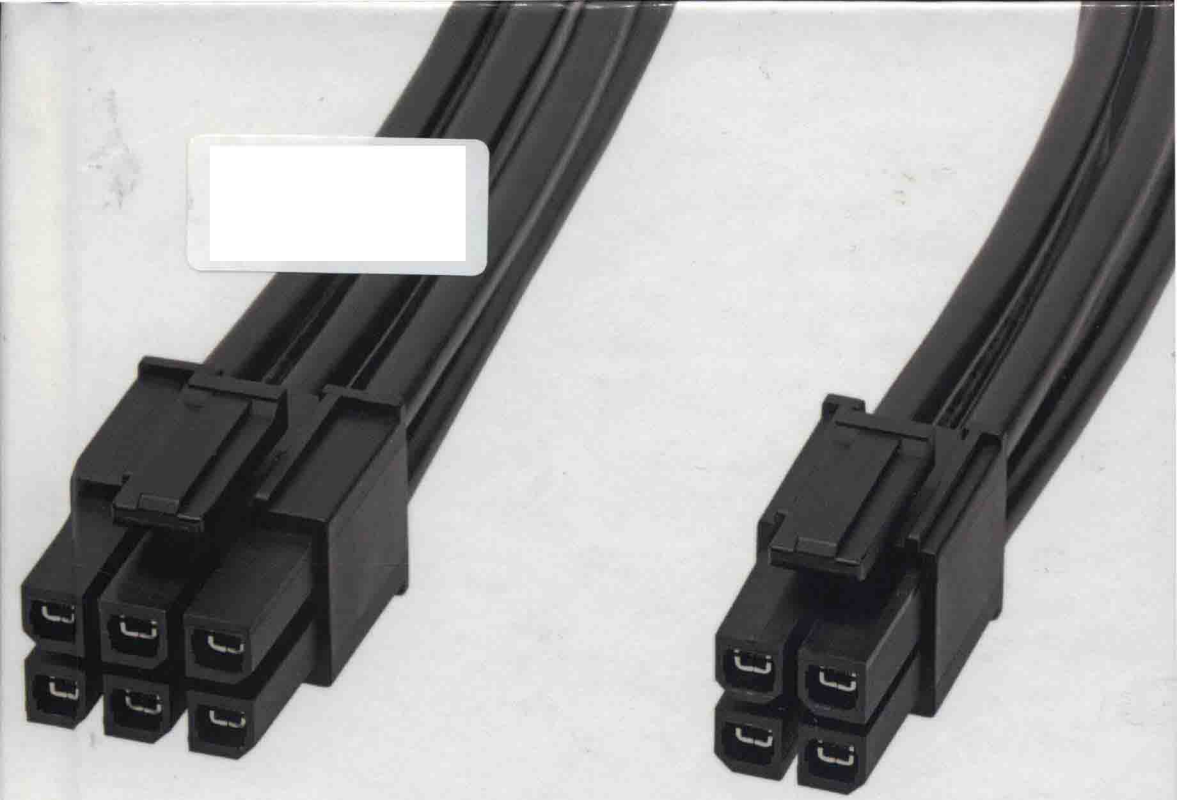

Optoelectronics Handbook

Rodney Lappin

Optoelectronics Handbook

Edited by **Rodney Lappin**

LANRYE INTERNATIONAL

New Jersey

Published by Clanrye International,
55 Van Reypen Street,
Jersey City, NJ 07306, USA
www.clanryeinternational.com

Optoelectronics Handbook
Edited by Rodney Lappin

International Standard Book Number: 978-1-63240-404-6 (Hardback)

Printed in the United States of America.

Optoelectronics Handbook

Preface

Over the recent decade, advancements and applications have progressed exponentially. This has led to the increased interest in this field and projects are being conducted to enhance knowledge. The main objective of this book is to present some of the critical challenges and provide insights into possible solutions. This book will answer the varied questions that arise in the field and also provide an increased scope for furthering studies.

Optoelectronics is intertwined with photonics. The book focuses on the study and function of electronic tools that release, identify and control light. As a field of study, it has flourished internationally and enabled many of the currently used conveniences. Because of this universality, novel functions and optical phenomena have led to further modernization. This book covers current achievements by experts around the world. A lot of developed and developing nations have contributed to this attempt. Chapters in this book are written by prominent scientists working in USA, Japan, India, as well as through the joint participation of the US and Moldova scientists. This book also describes properties and applications of optoelectronic devices employing organic and inorganic substances.

I hope that this book, with its visionary approach, will be a valuable addition and will promote interest among readers. Each of the authors has provided their extraordinary competence in their specific fields by providing different perspectives as they come from diverse nations and regions. I thank them for their contributions.

Editor

Contents

Chapter 1

ZnO-Based Light-Emitting Diodes

J.C. Fan, S.L. Chang and Z. Xie

Additional information is available at the end of the chapter

1. Introduction

In the past decade, light-emitting diodes (LEDs) based on wideband gap semiconductor have attracted considerable attention due to its potential optoelectronic applications in illumination, mobile appliances, automotive and displays [1]. Among the available wide band gap semiconductors, zinc oxide, with a large direct band gap of 3.37eV, is a promising candidate because of characteristic features such as a large exciton binding energy of 60meV, and the realization of band gap engineering to create barrier layers and quantum wells with little lattice mismatch. ZnO crystallizes in the wurtzite structure, the same as GaN, but, in contrast, large ZnO single crystal can be fabricated [2]. Furthermore, ZnO is inexpensive, chemically stable, easy to prepare and etch, and nontoxic, which also make the fabrication of ZnO-based optical devices an attractive prospect. The commercial success of GaN-based optoelectronic and electronic devices trig the interest in ZnO-based devices [2-4].

Recently, the fabrication of *p*-type ZnO has made great progress by mono-doping group V elements (N, P, As, and Sb) and co-doping III–V elements with various technologies, such as ion implantation, pulsed laser deposition (PLD), molecular beam epitaxy (MBE) [2,3]. A number of researchers have reported the development of homojunction ZnO LEDs and heterojunction LEDs using *n*-ZnO deposited on *p*-type layers of GaN, AlGaN, conducting oxides, or *p*-ZnO deposited on a *n*-type layer of GaN [1,3].

Figure1a shows the schematic structure of a typical ZnO homostructural p–i–n junction prepared by Tsukaza et al [5]. The I-V curve of the device displayed the good rectification with a threshold voltage of about 7V (Figure1b). The electroluminescence (EL) spectrum from the p–i–n junction (blue) and photoluminescence (PL) spectrum of a p-type ZnO film at 300K were shown in Figure1c, which indicated that ZnO was a potential material for making short-wavelength optoelectronic devices, such as LEDs for display, solid-state illumination and photodetector.

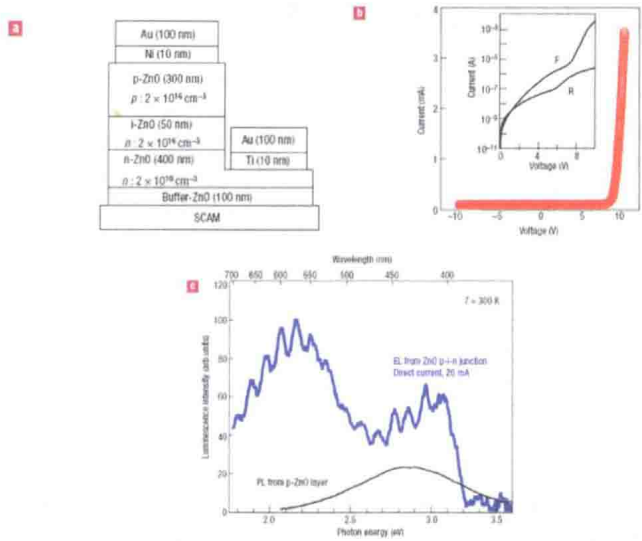

Figure 1. ZnO homostructural p–i–n junction shows rectifying current–voltage characteristics and electroluminescence (EL) in forward bias at room-temperature. (a), The structure of a typical p–i–n junction LED. (b), Current–voltage characteristics of a p–i–n junction. The inset has logarithmic scale in current with F and R denoting forward and reverse bias conditions, respectively. (c), Electroluminescence spectrum from the p–i–n junction (blue) and photoluminescence (PL) spectrum of a p-type ZnO film measured at 300 K. The p–i–n junction was operated by feeding in a direct current of 20 mA. From Ref.[5].

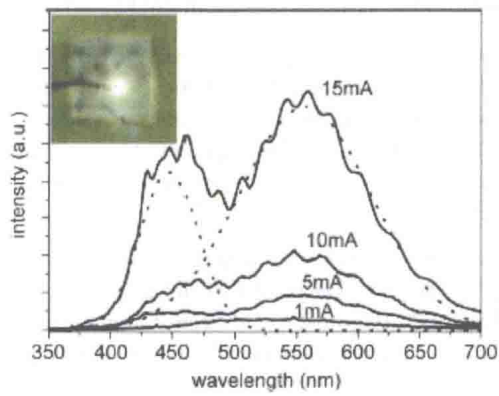

Figure 2. Room-temperature EL spectra of the n-ZnO/p-GaN heterojunction LED measured at various dc injection currents from 1 to 15mA at reverse breakdown biases. (Inset) EL image of the LED in a bright room. From Ref. [6].

White-light electroluminescence from n-ZnO)/p-GaN heterojunction LED was reported [6]. The spectrum range from 400 to 700nm is caused by the carrier recombination at the interface between n-ZnO and p-GaN, as shown in Figure2, which makes ZnO as a strong candidates for solid-state light.

Currently, ZnO-based LEDs are leaping from lab to factory. A dozen or so companies are developing ultraviolet and white LEDs for market. The coloured ZnO-based LEDs have been produced by Start-up company MOXtronics, which shows its full-colour potential. Although the efficiency of these LEDs is not high, improvements are rapid and the emitters have the potential to outperform their GaN rivals. Figure3 shows some EL images of ZnO-based LEDs.

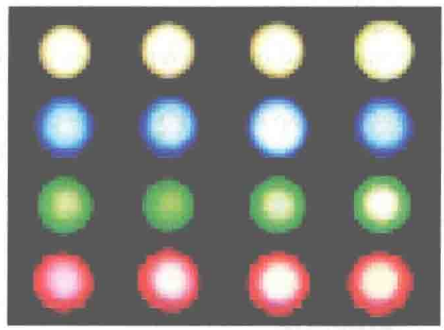

Figure 3. Some EL images of ZnO-based LEDs. From Ref. [7].

In this paper, based on the introduction of the band-gap engineering and doping in ZnO, we discuss the ZnO-based LEDs, comprehensively. We first discuss the band-gap engineering in ZnO, which is a very important technique to design ZnO-based LEDs. We then present the p- and n-types doping in ZnO. High quality n-type and/or p-type ZnO are necessary to prepare ZnO-based LEDs. Finally, we review the ZnO-based LEDs. In this part, we discuss homojunction ZnO LEDs and heterojunctions LEDs using *n*-ZnO deposited on *p*-type layers (GaN, AlGaN, conducting oxides, et al) or *p*-ZnO deposited on a *n*-type layer (GaN, Si, et al), comprehensively.

2. Band gap engineering in ZnO

Band gap engineering is the process of controlling or altering the band gap of a material by controlling the composition of certain semiconductor alloys. It is well known that tailoring of the energy band gap in semiconductors by band-gap engineering is important to create barrier layers and quantum wells with matching material properties, such as lattice constants, electron affinity for heterostructure device fabrication [2, 3].

Band-gap engineering in ZnO can be achieved by alloying with MgO, CdO or BeO. The energy band gap Eg(x) of ternary semiconductor $A_xZn_{1-x}O$ (A = Mg, Cd or Be) can be calculated by the following equation:

$$Eg(x) = (1- x)\, E_{ZnO} + x_{EAO} - bx\,(1 - x) \quad (1)$$

where b is the bowing parameter and E_{AO} and E_{ZnO} are the band-gap energies of compounds AO and ZnO, respectively. While adding Mg or Be to ZnO results in an increase in band gap, and adding Cd leads to a decrease in band gap [3, 8].

Both MgO and CdO have the rock-salt structure, which is not the same as the ZnO wurtzite structure. When Mg and Cd contents in ZnO are high, phase separation may be detected, while BeO and ZnO share the same wurtzite structure and phase separation is not observed in BeZnO [2, 8]. Ryu et al studied the band gap of BeZnO and did not observed any phase separation when Be content was varied over the range from 0 to 100mol%. Figure4 shows the a lattice parameter as a function of room-temperature Eg values in $A_xZn_{1-x}O$ alloy. Therefore, theoretically, the energy band gap of $A_xZn_{1-x}O$ can be continuously modulated from 0.9eV (CdO) to 10.6eV (BeO) by changing the A concentration [8]. Han et al reported the band gap energy of the $Be_xZn_{1-x}O$ can be tailored from 3.30eV (x = 0) to 4.13eV (x = 0.28) by alloying ZnO with BeO [9].

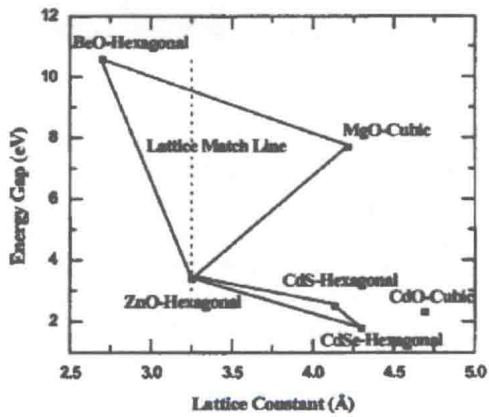

Figure 4. Energy band gaps, lattice constants and crystal structures of selected II-VI compounds. From Ref. [9].

Ohtomo et al investigated the band gap of $Mg_xZn_{1-x}O$ films grown on sapphire by PLD, where x is the atomic fraction [10]. The band gap of $Mg_xZn_{1-x}O$ could be increased to 3.99eV at room temperature as the content of Mg was increased upward to $x = 0.33$. Above 33%, the phase segregation of MgO impurity was observed from the wurtzite MgZnO lattice. Takagi et al reported the growth of wurtzite MgZnO film with Mg concentration of 51% on sapphire by molecular-beam epitaxy [11]. The band gap energy of $Mg_xZn_{1-x}O$ was successfully

turned from 3.3 to 4.5eV with the increase of Mg contents from 0 to 0.5. Tampo et al investigated excitonic optical transition in a $Zn_{1-x}Mg_xO$ alloy grown by radical source molecular beam epitaxy [12]. The strong reflectance peaks at room temperature were detected from 3.42eV (x=0.05) to 4.62eV (x = 0.61) from ZnMgO layers at room temperature. PL spectra at room temperature were also observed for energies up to 4.06eV (x = 0.44). Wassner et al studied the optical and structural properties of MgZnO films with Mg contents between x = 0 and x = 0.37 grown on sapphire by plasma assisted molecular beam epitaxy using a MgO/ZnMgO buffer layer [13]. In their experiments, the a-lattice parameter was independent from the Mg concentration, whereas the c-lattice parameter decreases from 5.20Å for x = 0 to 5.17Å for x = 0.37, indicating pseudomorphic growth. The peak position of the band edge luminescence blue shifted up to 4.11eV for x = 0.37.

Makino et al investigated the structure and optical properties of $Cd_xZn_{1-x}O$ films grown on sapphire (0001) and $ScAlMgO_4$ substrates by PLD [14]. The band gap of $Cd_xZn_{1-x}O$ films was estimated by $Eg(y) = 3.29 - 4.40y + 5.93y^2$. The band gap narrowing to 2.99eV was achieved by incorporating Cd^{2+} with Cd concentration of 7%. Both lattice parameters a and c increase with the increasing Cd content in ZnO, which was agreement with the larger atomic size of Cd compared with Zn. $Cd_xZn_{1-x}O$ films were also prepared on c-plane sapphires by metal-organic vapor-phase epitaxy. The fundamental band gap was narrowed up to 300meV for a maximum Cd concentration of ~5%, introducing a lattice mismatch of only 0.5% with respect to binary ZnO. Lai et al prepared the $Cd_xZn_{1-x}O$ alloy by conventional solid-state reaction over the composition range and found that CdO effectively decreased the electronic bandgap both in the bulk and near the surface ZnO [15].

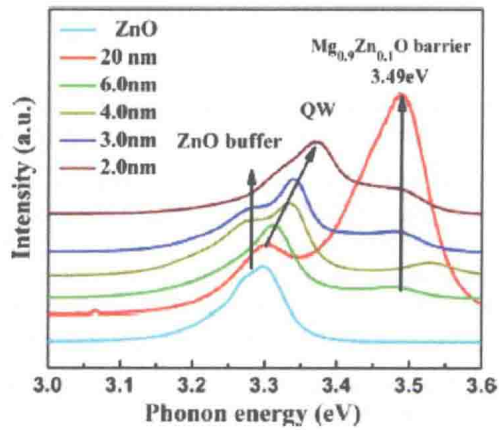

Figure 5. Room temperature PL spectra of $ZnO/Zn_{0.9}Mg_{0.1}O$ SQW with different well width. From Ref. [17].

Using MgZnO as barrier layers, Chauveau et al prepared the nonpolar a-plane (Zn,Mg)O/ZnO quantum wells (QWs) grown by molecular beam epitaxy on r plane sapphire and a plane ZnO substrates [16]. They observed the excitonic transitions were strongly blue-shifted due to the

anisotropic strain state in heteroepitaxial QW and the reduction of structural defects and the improvement of surface morphology were correlated with a strong enhancement of the photoluminescence properties. Su et al investigated the optical properties of ZnO/ZnMgO single quantum well (SQW) prepared by plasma-assisted molecular beam epitaxy [17]. The photoluminescence peak of the SQW shifted from 3.31 to 3.37eV as the well layer thickness was decreased from 6 to 2nm (Figure5). ZnO/MgZnO superlattices were also fabricated by laser molecular-beam epitaxy and the excitonic stimulated emission up to 373K was observed in the superlattices. The emission energy could be tuned between 3.2 and 3.4eV, depending on the well thickness and/or the Mg content in the barrier layers.

3. Doping in ZnO

ZnO has a strong potential for various short-wavelength optoelectronic device applications. To realize these applications, the reliable techniques for fabricating high quality n-type and p-type ZnO need to be established. Undoped ZnO exhibits n-type conduction due to the intrinsic defects, such as the Zinc interstitial (Zn_i) and oxygen vacancy (V_O). It is easy to obtain the high quality n-type ZnO material by doping group-III elements. However, it is a major challenge to dope ZnO to produce p-type semiconductor due to self-compensation from native donor defects and/or hydrogen incorporation. To achieve p-type ZnO, various elements (N, P, As, Sb and Li) have been tried experimentally as p-type dopants with various techniques, such as pulse laser deposition, magnetron sputtering, chemical vapor deposition (CVD), molecular-beam epitaxy, hybrid beam deposition (HBD), metal organic chemical vapor deposition (MOCVD) and thermal oxidation of Zn_3N_2 [2, 3].

3.1. n-type ZnO

A number of researchers investigated the electrical and optical properties of n-type ZnO materials by doping III elements, such as Al, Ga and In, which can easily substitute Zn ions [1-3].

Kim et al reported the high electron concentration and mobility in AZO films grown on sapphire by magnetron sputtering [18]. AZO films exhibited the electron concentrations and mobilities were of the order of $10^{18}cm^3$ and less than $8cm^2/Vs$, respectively, however, when annealed at 900^0C, the films showed remarkably improved carrier concentrations and mobilities, e.g., about 10^{20} cm^3 and 45 – 65 cm^2/Vs, respectively. Other researchers also reported the improved electrical properties in Al-doped zinc oxide by thermal treatment [19].

Bhosle et al investigated the electrical properties of transparent Ga-doped ZnO films prepared by PLD [20]. Temperature dependent resistivity measurements for the films showed a metal-semiconductor transition, which was rationalized by localization of degenerate electrons. The lowest value of resistivity 1.4×10^{-4} Ωcm was found at 5% Ga. Yamada et al reported the low resistivity Ga-doped ZnO films prepared on glass by ion plating with direct current arc discharge [21]. The ZnO:Ga film with a thickness of 98nm, exhibited a resistivity of 2.4×10^{-4} Ω cm, a carrier concentration of $1.1\times10^{21}cm^{-3}$ and a Hall mobility of $23.5cm^2/Vs$. Liang et al reported the Ga-doped ZnO films prepared on

glass by magnetron sputtering and found that a carrier concentration exhibited only a slight change with the thickness variations [22].

Wang et al studied the properties of In-doped ZnO crystal by the hydrothermal technique [23]. The indium-doped ZnO crystals have a resistivity lower than 0.015Ωcm with a free carrier concentration (mostly due to indium donors) of $1.09\times10^{19}/cm^3$ at room temperature. Quang et al reported the In-doped ZnO films grown by hydrothermal [24]. The films had a mobility of 4.18-20.9cm^2/Vs and a concentration of 6.7×10^{18} - $3.2\times10^{19}/cm^3$. The In-doped ZnO films with a carrier concentration of $3.22\times10^{20}/cm^3$ were grown by sol–gel method [25].

VII elements such as F and Cl are also used as n-type dopants in ZnO, which substituted oxygen ions. Cao et al reported F-doped ZnO grown by PLD with a minimum resistivity of 4.83×10^{-4} Ωcm, with a carrier concentration of $5.43\times10^{20}cm^{-3}$ and a mobility of 23.8cm^2/ Vs [26]. Chikoidze et al grew Cl-doped ZnO films by MOCVD with a resistivity of 3.6×10^{-3} Ω cm [27].

3.2. p-type ZnO

To realize ZnO-based LEDs, the most important issue is the fabrication of high quality p-type ZnO. However, undoped ZnO exhibits n-type conduction and the reliable p-type doping of the materials remains a major challenge because of the self-compensation from native donor defects (Vo and Zn_i) and/or hydrogen incorporation. Considerable efforts have been made to obtain p-type ZnO by doping different elements (N, P, As, Sb, Li, Na and K) with various techniques [2, 3]. Here, we present the typical results of p-type ZnO materials.

Among all potential p-type dopants for ZnO, N is considered the most promising dopant due to similar ionic radius compared with oxygen. It substitutes O sites in ZnO structure, resulting in the shallow acceptors. N_2, NO, N_2O, NH_3 and Zn_3N_2 are acted as N sources depended on growth techniques [2, 3]. Liu et al reported p-type ZnO:N films grown on c-sapphire by plasma-assisted molecular beam epitaxy [28]. The anomalous Raman mode at 275cm^{-1} was confirmed to be related to substitution of N for O site (N_O) in ZnO. The films exhibited a hole concentration of $2.21\times10^{16}cm^{-3}$ and a mobility of 1.33cm^2/Vs. Zeng et al investigated p-type ZnO films prepared on a-plane (11–20) sapphire by MOCVD [29]. The optimized result was achieved at the temperature of 400°C with a resistivity of 1.72Ωcm, a Hall mobility of 1.59cm^2/Vs, and a hole concentration of $2.29\times10^{18}cm^{-3}$. Wang et al prepared p-type ZnO films by oxidation of Zn_3N_2 films grown by direct current magnetron sputtering [30]. For oxidation temperature between 350 and 500°C, p-type ZnO:N films were achieved, with a hole concentration of $5.78\times10^{17}cm^{-3}$ at 500°C. Kumar et al reported on the growth of p-type N,Ga-codoped ZnO films prepared by sputtering ZnO:Ga_2O_3 target in N_2O ambient [31]. The film deposited on sapphire at 550°C exhibited p-type conduction with a hole concentration of 3.9×10^{17} cm^{-3}.

Beside N, other group V elements (P, As and Sb) are also used to be acceptor dopants to obtain p-type ZnO. However, first-principle calculations show that X_O (P_O, As_O and Sb_O) are deep acceptors and have high acceptor-ionization energies, owing to their large ionic radii as compared to O, which make it impossible for X_O to dop ZnO efficiently p-type [32]. We

could not contribute the p-type behavious in X doped ZnO to X_O, simply. Recently, for the large-size-mismatched impurities in ZnO, Limpijumnong et al proposed X_{Zn}–$2V_{Zn}$ acceptor model [33]. In the model, X substitute Zn sites, forming a donor, then it induces two Zn vacancy acceptors as a complex form X_{Zn}–$2V_{Zn}$. The ionization energy of As_{Zn} - $2V_{Zn}$ complex was calculated to be 0.15eV (0.16eV for Sb_{Zn} – $2V_{Zn}$).

Xiu et al reported p-type P-doped ZnO films grown by MBE using a GaP effusion cell as a phosphorus dopant source [34]. PL spectra clearly indicated the existence of competitions between D^0X and A^0X for the phosphorus-doped ZnO films. The films exhibited a carrier concentration of 6.0×10^{18} cm^{-3}, Hall mobility of 1.5 cm^2/Vs, and resistivity of 0.7Ωcm. Kim et al achieved p-type ZnO:P films on a sapphire substrate using phosphorus doping and a thermal annealing process [35]. As-grown n-type ZnO:P prepared by radio-frequency sputtering were converted to *p*-ZnO:P by an rapid thermal annealing process under a N_2 ambient. The films had a hole concentration of 1.0×10^{17} – 1.7×10^{19}/cm^3, a mobility of 0.53 – 3.51cm^2/Vs and a resistivity of 0.59 – 4.4 Ωcm. Pan et al prepared p-type ZnO:P films on the insulating quartz with a hole concentration of 1.84×10^{18} cm^{-3} by MOCVD [36]. Vaithianathan et al grew p-type ZnO:P films on Al_2O_3(0001) by PLD [37]. The films exhibited a hole concentration of 5.1×10^{14} –$1.5\times10^{17}$$cm^{-3}$, a hole mobility of 2.38 – 39.3 cm^2 / V s, and a resistivity of 17 – 330 Ωcm.

Ryu et al investigated the electrical properties of As-doped ZnO films on O–ZnO substrates by hybrid beam deposition [38]. The electrical behavior of ZnO:As films changed from intrinsic *n*-type to highly conductive *p*-type with increased As dopant concentration. They achieved p-type ZnO:As films with a hole concentration of 4×10^{17} cm^{-3} and a mobility of 35cm^2/Vs. Vaithianathan et al reported As-doped p-type ZnO films using a Zn_3As_2 /ZnO target by PLD [39]. As-grown ZnO:As showed n-type conductivity, however, ZnO:As films after annealed at 200°C in N_2 ambient for 2 min exhibited *p*-type conductivity with the hole concentrations varied between 2.48×10^{17} and $1.18\times10^{18}$$cm^{-3}$. Kang et al grew ZnO films on GaAs by sputtering and annealed at 500°C in an oxygen gas pressure of 40 mTorr for 20 min. After annealing, ZnO film on GaAs showed *p*-type conductivity with a hole concentration of $9.684\times10^{19}$$cm^{-3}$, a mobility of 25.37$cm^2$/Vs, and a resistivity of 2.54 $\times10^{-3}$ Ωcm. The acceptor binding energy was calculated to be 0.1445eV, which was in good agreement with the ionization energy of As_{Zn} - $2V_{Zn}$ acceptor complex (0.15eV) [40].

Guo et al reported p-type ZnO:Sb films grown by PLD [41]. The films showed a resistivity of 4.2 – 60Ωcm, a Hall mobility of 0.5 – 7.7cm^2/V s, and a hole concentration of $1.9–2.2\times10^{17}$$cm^{-3}$. In the (HR) TEM images of p-type ZnO:Sb, they observed a high density of threading dislocations originating from the film/substrate interface and a large number of partial dislocation loops associated with small stacking faults. Xiu et al fabricated p-type ZnO:Sb films grown on n-Si (100) by MBE [42]. The film had a concentration of 1.7×10^{18} cm^{-3}, and a high mobility of 20.0cm^2/Vs and a low resistivity of 0.2Ωcm. The acceptor energy level of the Sb dopant was about 0.2eV above the valence band, which was agreement with the ionization energy of Sb_{Zn} – $2V_{Zn}$ (0.16eV).

Some researchers prepared p-type ZnO using Group I elements (Li, Na and K) as acceptor dopants. Yi et al fabricated p-type ZnO:Li films grown on quartz substrate by PLD